

## Supporting Information

### **A novel A-DA'D-A bifunctional small molecule for organic solar cells application with impressive photovoltaic performance**

Junfang Lv,<sup>a</sup> Yuhao Chen,<sup>a</sup> Xia Guo,<sup>a</sup> Jinjing Qiu,<sup>a</sup> Zhiliang Zhang,<sup>a</sup> Jianqiu Wang,<sup>a</sup> Haiyan Liang,<sup>a</sup> Liu Zhang,<sup>a</sup> Lei Zhu,<sup>b</sup> Feng Liu,<sup>b</sup> Maojie Zhang\*<sup>a</sup>

<sup>a</sup>Laboratory of Advanced Optoelectronic Materials, Suzhou Key Laboratory of Novel Semiconductor-optoelectronics Materials and Devices, College of Chemistry, Chemical Engineering and Materials Science, Soochow University, Suzhou 215123, China

E-mail: mjzhang@suda.edu.cn.

<sup>b</sup>Frontiers Science Center for Transformative Molecules, School of Chemistry and Chemical Engineering, Shanghai Jiao Tong University, Shanghai 200240, P. R. China

### **Experimental Section**

#### **<sup>1</sup>H NMR, <sup>13</sup>C NMR, TGA, and DSC measurement**

<sup>1</sup>H NMR and <sup>13</sup>C NMR spectra were measured in CDCl<sub>3</sub> on Bruker AV 400 MHz FT-NMR spectrometer. Thermogravimetric analysis (TGA) was performed on a Perkin–Elmer TGA–7. Differential scanning calorimetry (DSC) was performed on a TA DSC Q-200.

#### **UV-vis absorption and Cyclic voltammetry**

UV-vis absorption spectra were taken on an Agilent Technologies Cary Series UV-Vis-NIR Spectrophotometer. The electrochemical cyclic voltammetry (CV) was performed on a Zahner Ennium IM6 Electrochemical Workstation with glassy carbon disk, Pt wire, and Ag/Ag<sup>+</sup> electrode as working electrode, counter electrode, and reference electrode respectively, in a 0.1 M tetrabutylammonium hexafluorophosphate (Bu<sub>4</sub>NPF<sub>6</sub>) acetonitrile solution.

#### **Device fabrication and characterization**

The Indium tin oxide (ITO)-coated glass substrates were pre-cleaned twice by sequential ultrasonication in deionized water and isopropanol for 15 min each. After 20 min of ultraviolet-ozone treatment, a thin layer of 30 nm thick PEDOT:PSS was spin-coated onto the substrates

as the anode interlayer and annealed at 150 °C for 15 min. The substrates were transferred into the nitrogen-filled glove box.

P3HT:BPM1 based devices were fabricated as following: the active layer solution was spin-coated on the PEDOT:PSS layer to form the 100 nm thick active layer. P3HT:BPM1 solution were prepared with a donor/acceptor (D/A) weight ratio of 1:1 in tetrahydrofuran at a total concentration of 20 mg mL<sup>-1</sup>. follow with thermal annealing at 130 °C for 10 min. Then PFN-Br methanol solution (0.5 mg mL<sup>-1</sup>) was spincoated on the active layer to give a 5 nm thick cathode interlayer. Finally, about 100 nm thick of Al was deposited onto the active layer under high vacuum, giving an effective cell area of 4 mm<sup>2</sup>.

BPM1:Y6 based devices were fabricated as following: the active layer solution was spin-coated on the PEDOT:PSS layer to form the 100 nm thick active layer. BPM1:Y6 solution were prepared with a donor/acceptor (D/A) weight ratio of 1:1 in chloroform at a total concentration of 20 mg mL<sup>-1</sup>. Follow with solvent vapor annealing by CS<sub>2</sub> for 90 s. Besides, 5 wt % PM7 as a solid additive was introduced into the BPM1:Y6 to improve the PCE. Then PFN-Br methanol solution (0.5 mg mL<sup>-1</sup>) was spincoated on the active layer to give a 5 nm thick cathode interlayer. Finally, about 100 nm thick of Al was deposited onto the active layer under high vacuum, giving an effective cell area of 4 mm<sup>2</sup>.

### ***J-V* and EQE measurement**

The current density–voltage (*J-V*) characteristics of the OSCs were recorded with a Keithley 2450. The power conversion efficiencies of the OSCs were measured under 1 sun, AM 1.5G (air mass 1.5 global) (100 mW cm<sup>-2</sup>) using a SS-F5-3A (Enli Technology CO., Ltd.) solar simulator (AAA grade, 50 mm × 50 mm photo-beam size). 2 × 2 cm<sup>2</sup> monocrystalline silicon reference cell (SRC-00019, covered with a KG5 filter windows) was purchased from Enli Technology CO., Ltd. The EQE was measured by solar cell spectral response measurement system QE-R3011 (Enli Technology CO., Ltd.). The light intensity at each wavelength was calibrated with a standard single-crystal Si photovoltaic cell.

## SCLC Mobility measurement

The hole and electron mobilities of devices were evaluated from space-charge-limited current (SCLC) method. The corresponding charge mobilities were calculated from fitting the Mott-Gurney square law  $J = 9\varepsilon_r\varepsilon_0\mu V^2/(8L^3)$ , where  $J$  is the current density,  $\varepsilon_r$  is the dielectric permittivity of the active layer (assumed to be 3),  $\varepsilon_0$  is the vacuum permittivity,  $L$  is the thickness of the active layer,  $\mu$  is the hole or electron mobility.  $V=V_{\text{appl}} - V_{\text{bi}} - V_s$ ,  $V_{\text{appl}}$  is the applied voltage,  $V_{\text{bi}}$  is the built-in voltage,  $V_s$  is the voltage drop from the substrate's series resistance ( $V_s = IR$ ). The SCLC devices were measured under dark condition in a nitrogen glovebox without encapsulation.

## $J_{\text{ph}}-V_{\text{eff}}$ measurement

Exciton dissociation efficiency ( $P_{\text{diss}}$ ) and charge collection efficiency ( $P_{\text{coll}}$ ) were measured to investigate the exciton dissociation and charge collection process in devices. According to previous literature,<sup>1-3</sup>  $P_{\text{diss}}$  is obtained in formula, as following:

$$P_{\text{diss}} = \frac{J_{\text{ph}}^*}{J_{\text{sat}}} \times 100\%$$

where  $J_{\text{sat}}$  is the saturated short-circuit current density and  $J_{\text{ph}}^*$  is the photo-current density under the short circuit condition. Besides,  $P_{\text{coll}}$  is also deduced from following formula,

$$P_{\text{coll}} = \frac{J_{\text{ph}}^{\&}}{J_{\text{sat}}} \times 100\%$$

where  $J_{\text{sat}}$  is the saturated short-circuit current density and  $J_{\text{ph}}^{\&}$  is the photo-current density under the maximal power output condition. Among them,  $J_{\text{ph}}$  is defined as  $J_L - J_D$ , where  $J_L$  and  $J_D$  are the current density under light irradiation and in the dark,<sup>4,5</sup> respectively. In addition, the saturation current density ( $J_{\text{sat}}$ ) is only limited by total amount of absorbed incident photons if we assume that all the photogenerated excitons are dissociated into free charge carriers and collected by electrodes at a high  $V_{\text{eff}}$ .<sup>6</sup>  $V_{\text{eff}}$  is defined as  $V_0 - V_{\text{bias}}$ , where  $V_0$  is the voltage when

$J_{\text{ph}} = 0$  and  $V_{\text{bias}}$  is the applied bias voltage.  $J_{\text{sat}}$ ,  $J_{\text{ph}}$  and  $V_{\text{eff}}$  are obtained by related testing. Finally, the  $P_{\text{diss}}$  and  $P_{\text{coll}}$  are calculated by the above formula, respectively.

### **TPC and TPV measurement**

Transient photovoltage (TPV) and transient photocurrent (TPC) measurements were carried out under a 337 nm 3.5 ns pulse laser (160  $\mu\text{J}$  per pulse at 10 Hz) and halide lamps (150 W). Voltage and current dynamics were recorded on a digital oscilloscope (Tektronix MDO3102).

### **AFM and TEM characterization**

Atomic force microscopy (AFM) measurements were performed on a Dimension 3100 (Veeco) Atomic Force Microscope in the tapping mode. Transmission electron microscopy (TEM) was performed using a Tecnai G2 F20 S-TWIN instrument at 200 kV accelerating voltage, in which the blend films were prepared as following: first, the blend films were spin-coated on the PEDOT:PSS/ITO substrates; second, the resulting blend film/PEDOT:PSS/ITO substrates were submerged in deionized water to make these blend films float onto the air-water interface; finally, the floated blend films were taken up on unsupported 200 mesh copper grids for a TEM measurement.

### **GIWAXS measurement**

Grazing incidence wide-angle X-ray scattering (GIWAXS) measurements were performed at beamline 7.3.3 at the Advanced Light Source, Molecular Foundry, Lawrence Berkeley National Laboratory, supported by the US Department of Energy, Office of Science, Office of Basic Energy Sciences. Samples were prepared on Si substrates using identical blend solutions as those used in devices. The 10 keV X-ray beam was incident at a grazing angle of  $0.12^\circ - 0.16^\circ$ , selected to maximize the scattering intensity from the samples. The scattered x-rays were detected using a Dectris Pilatus 2M photon-counting detector. Besides, the CCL is calculated by the Scherrer equation.<sup>7</sup>

### **Contact Angle measurement**



poured into methanol and filtered. The residue was purified with column chromatography on silica gel using dichloromethane/petroleum ether (1/1, v/v) as the eluent to give a dark aubergine solid BPM1 (0.16 g, 78%).  $^1\text{H}$  NMR (400 MHz,  $\text{CDCl}_3$ )  $\delta$  8.08 (s, 2H), 4.72-4.65 (t, 4H), 4.16-4.18 (d, 4H), 3.07-3.03 (t, 4H), 2.04-2.01 (t, 2H), 1.88-1.83 (t, 4H) 1.75-1.70 (t, 4H), 1.47-0.85 (m, 64H), 0.72-0.63 (m, 12H).  $^{13}\text{C}$  NMR (101 MHz,  $\text{CDCl}_3$ )  $\delta$  192.04, 167.73, 147.51, 144.16, 143.36, 136.93, 132.66, 132.35, 127.81, 126.17, 124.15, 118.59, 112.41, 77.37, 77.25, 77.05, 76.73, 55.21, 44.75, 40.27, 31.93, 30.04, 29.73, 29.66, 29.63, 29.56, 29.45, 29.36, 29.15, 28.70, 27.91, 27.83, 23.28, 23.22, 22.80, 22.72, 20.14, 14.16, 13.87, 13.76, 10.24, 10.15. HR-MS (MALDI-TOF)  $m/z$  calcd. for ( $\text{C}_{58}\text{H}_{82}\text{N}_4\text{O}_2\text{S}_5$ ): 1368.5. Found: 1368.46.

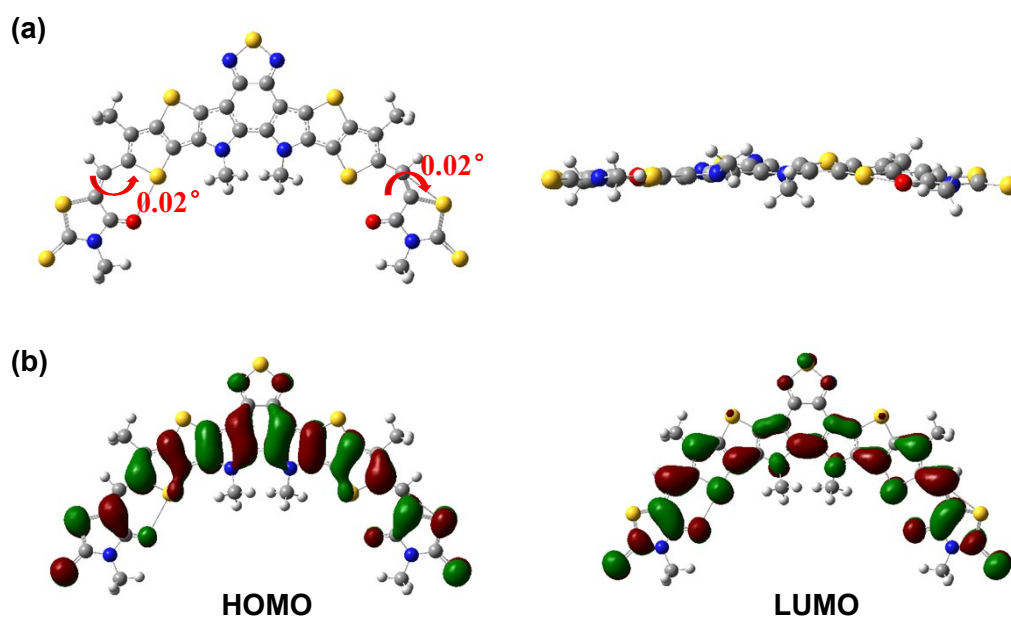


**Fig. S1** (a) Top view and side view of the optimized geometry of BPM1. (b) the frontier molecular orbital of HOMO and LUMO of BPM1.

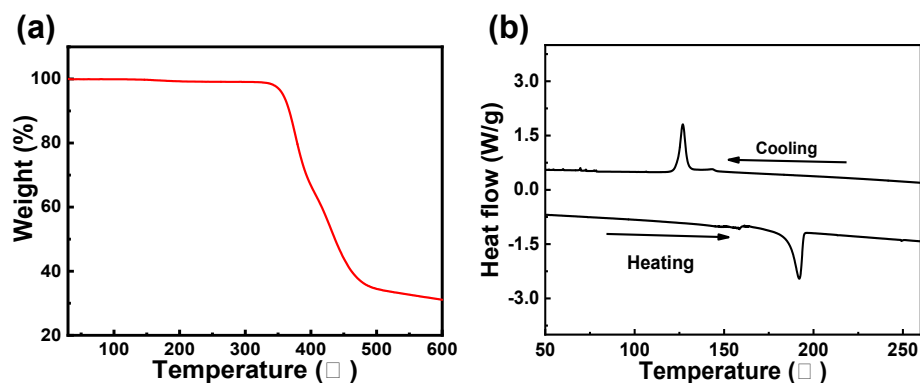


**Fig. S2** (a) The TGA and (b) DSC curve of BPM1 at a scan rate of  $10\text{ }^{\circ}\text{C min}^{-1}$  under nitrogen.

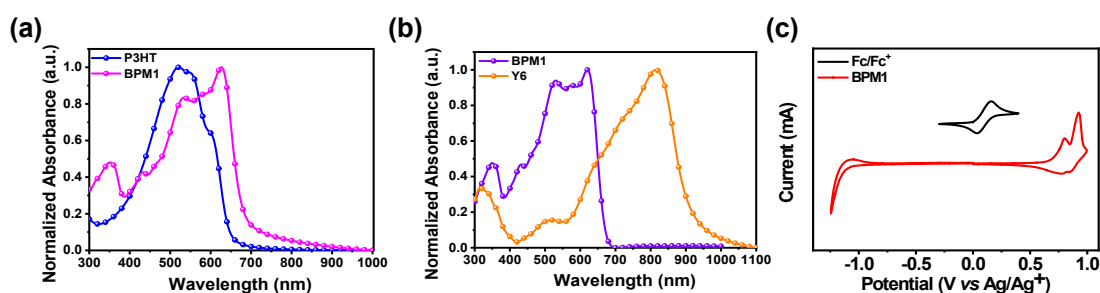


**Fig. S3** (a) The absorption of BPM1 and P3HT in thin film. (b) The absorption of BPM1 and Y6 in thin film. (c) Cyclic voltammogram of BPM1 film on a glassy carbon electrode measured in  $0.1\text{ mol L}^{-1}$  Bu<sub>4</sub>NPF<sub>6</sub> acetonitrile solution at a scan rate of  $50\text{ mVs}^{-1}$

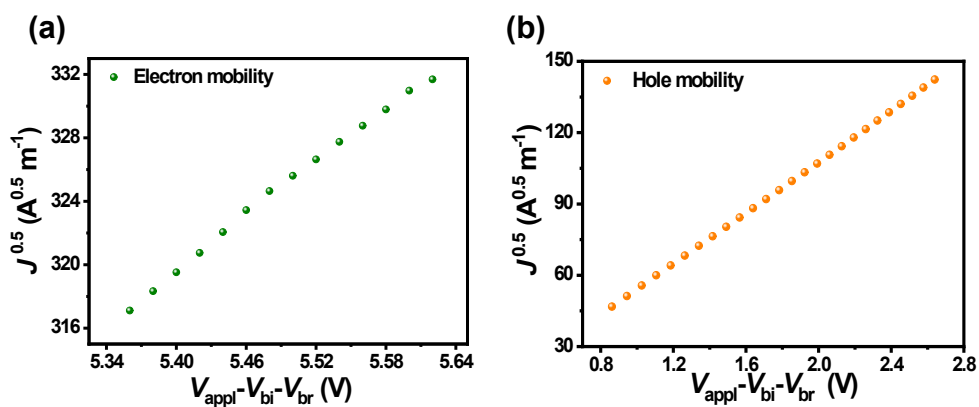


**Fig. S4** (a) The  $J^{0.5}$ - $V$  plot of electron-only and (b) hole-only devices based on BPM1 neat film.

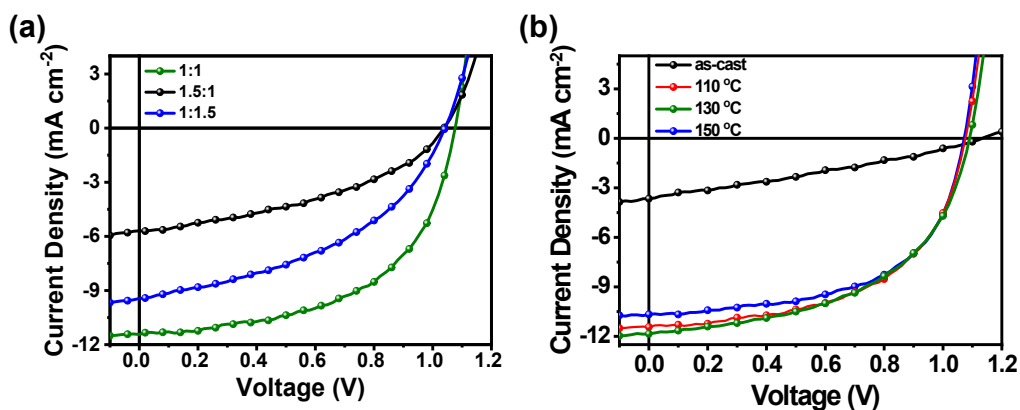


**Fig. S5** (a)  $J$ - $V$  curves of the OSCs based on P3HT:BPM1 with different D/A weight ratios (TA at 130 °C for 10 min). (b)  $J$ - $V$  curves of the OSCs based on P3HT:BPM1 with as-cast and with different TA temperature.

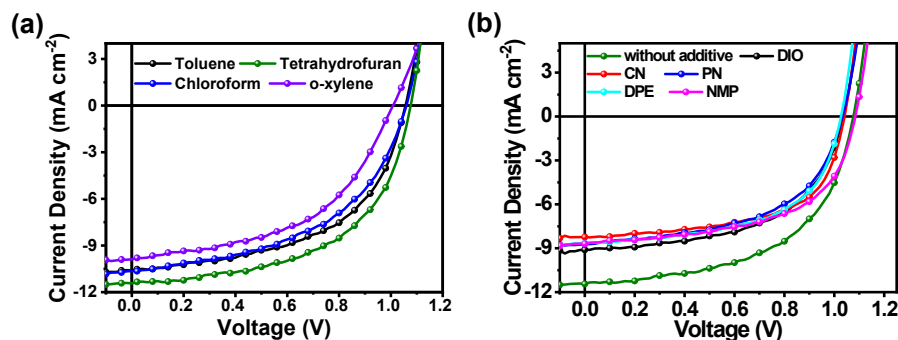


**Fig. S6** (a)  $J$ - $V$  curves of P3HT:BPM1 OSCs with different solvent (TA at 130 °C for 10 min). (b)  $J$ - $V$  curves of P3HT:BPM1 OSCs with different additive (TA at 130 °C for 10 min).

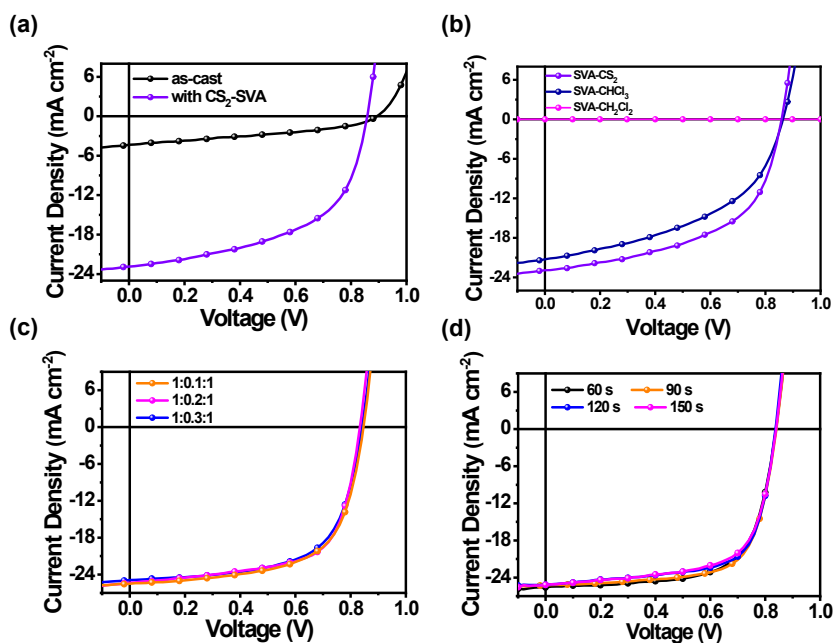


**Fig. S7** (a)  $J$ - $V$  curves of BPM1:Y6 OSCs under as-cast and CS<sub>2</sub>-SVA-90 s. (b)  $J$ - $V$  curves of BPM1:Y6 OSCs with SVA under different solvents. (c) The  $J$ - $V$  curves of the BPM1:Y6 blend



with different PM7 content (CS<sub>2</sub>-SVA-90 s). (d)  $J$ - $V$  curves of BPM1:PM7:Y6 OSCs with different time under the condition of SVA treatment.

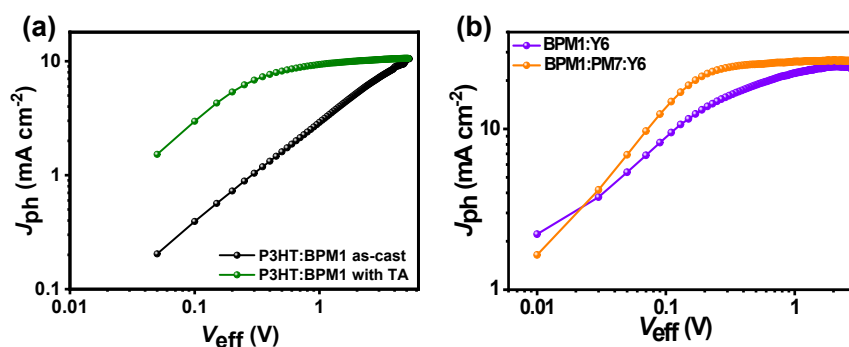


**Fig. S8** (a) and (b) the plots of photocurrent ( $J_{ph}$ ) versus effective voltage ( $V_{eff}$ ) curves of P3HT:BPM1, BPM1:Y6, BPM1:PM7:Y6.

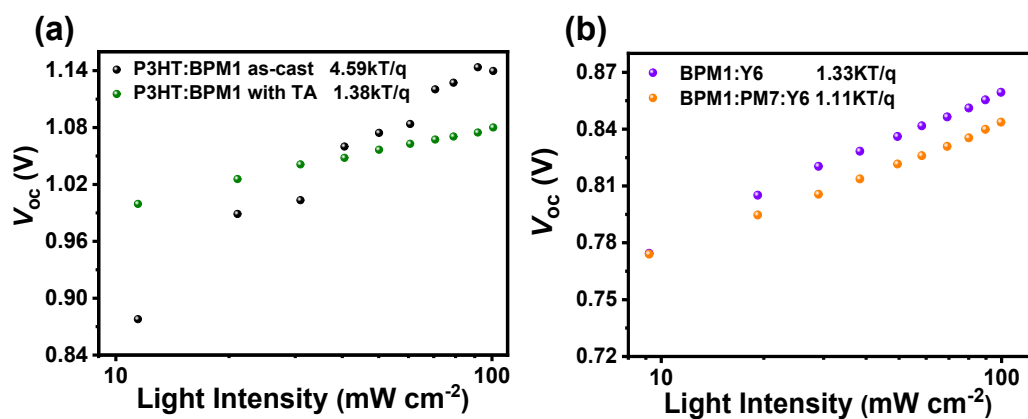


**Fig. S9** (a) and (b) The dependence of  $V_{oc}$  on light intensity of corresponding OSCs.

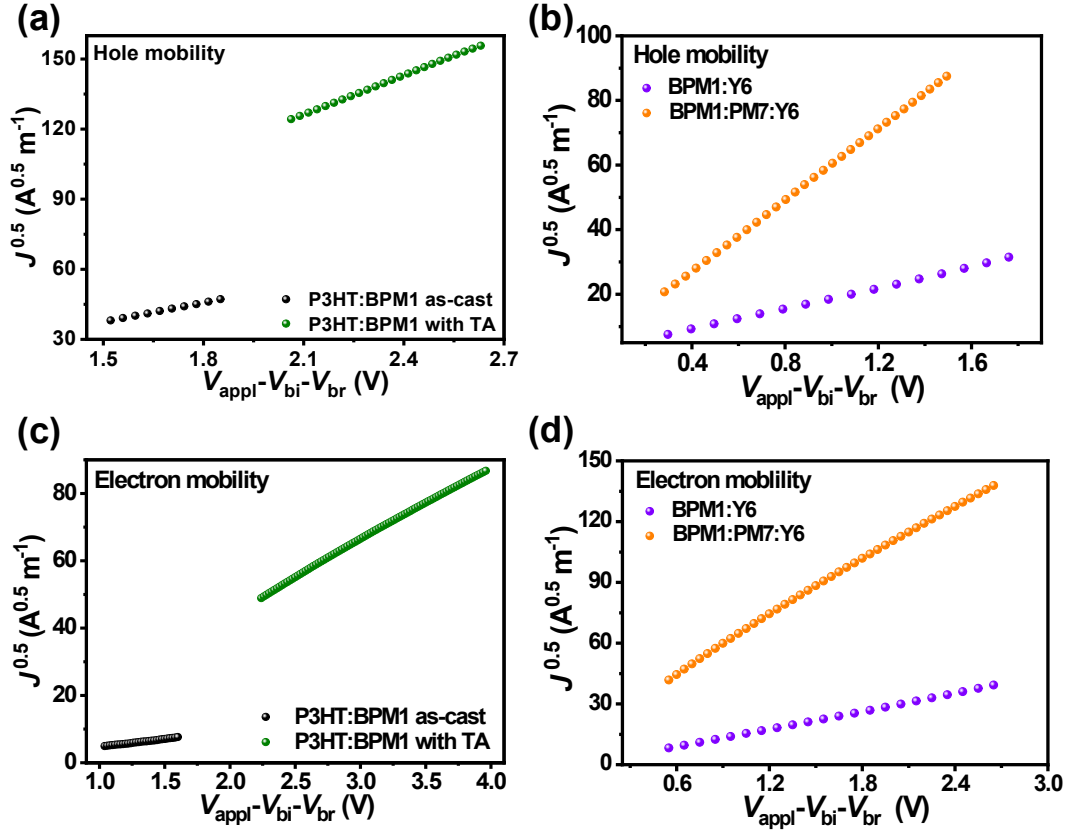


**Fig. S10** (a-b) The  $J^{0.5}$ - $V$  plots of hole-only and (c-d) electron-only based on corresponding OSCs.

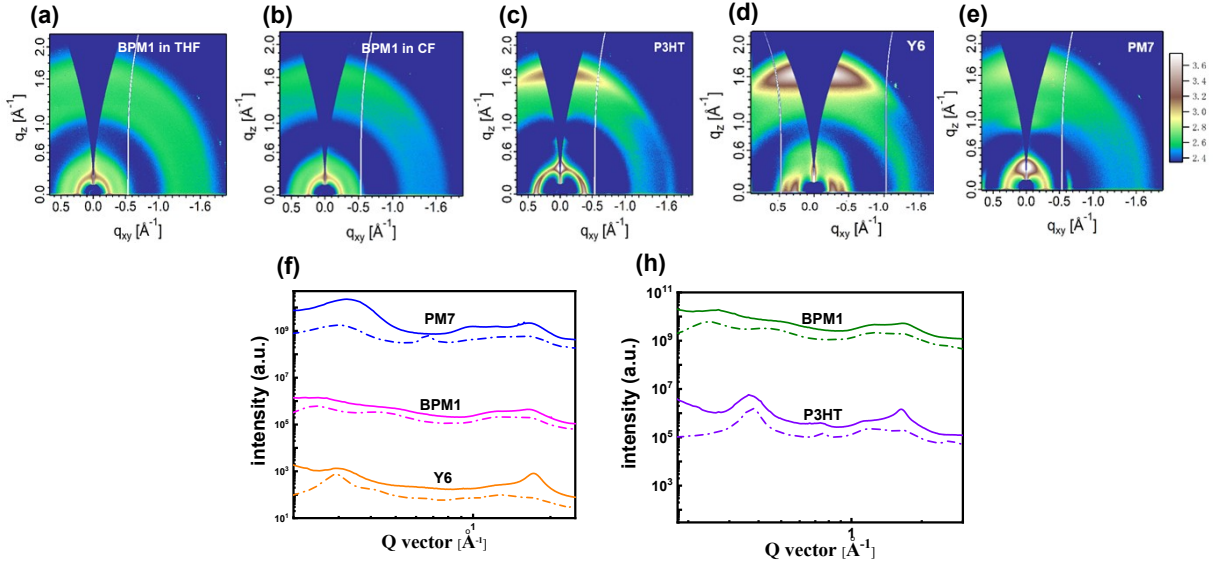


**Fig. S11** (a-e) 2D GIWAXS patterns of BPM1, P3HT, Y6 and PM7. (f) the line-cut profiles of neat film in the IP (dash line) and OOP (solid line) directions of corresponding neat film in CF. (h) the line-cut profiles of neat film in the IP (dash line) and OOP (solid line) directions of corresponding neat film in THF.

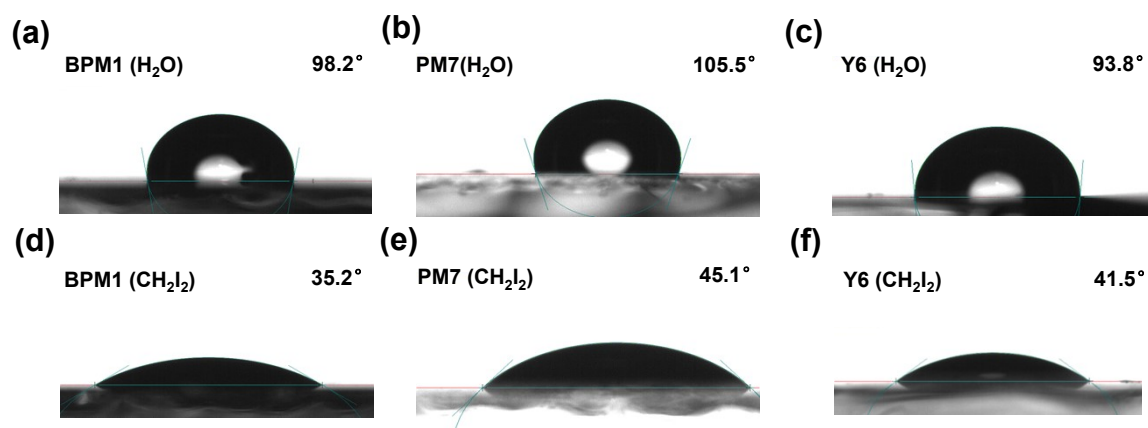


Fig. S12 Contact angles measurement of BPM1, Y6 and PM7 neat film.

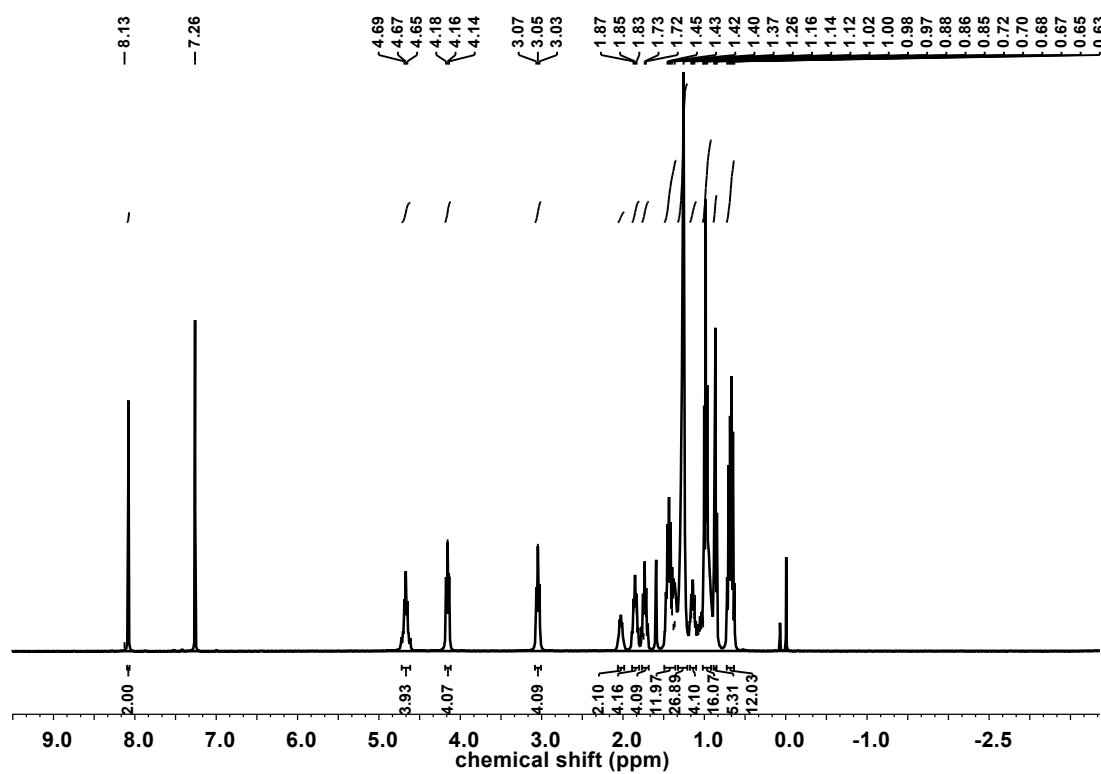


Fig. S13 <sup>1</sup>H NMR spectra of BPM1 in CDCl<sub>3</sub>.

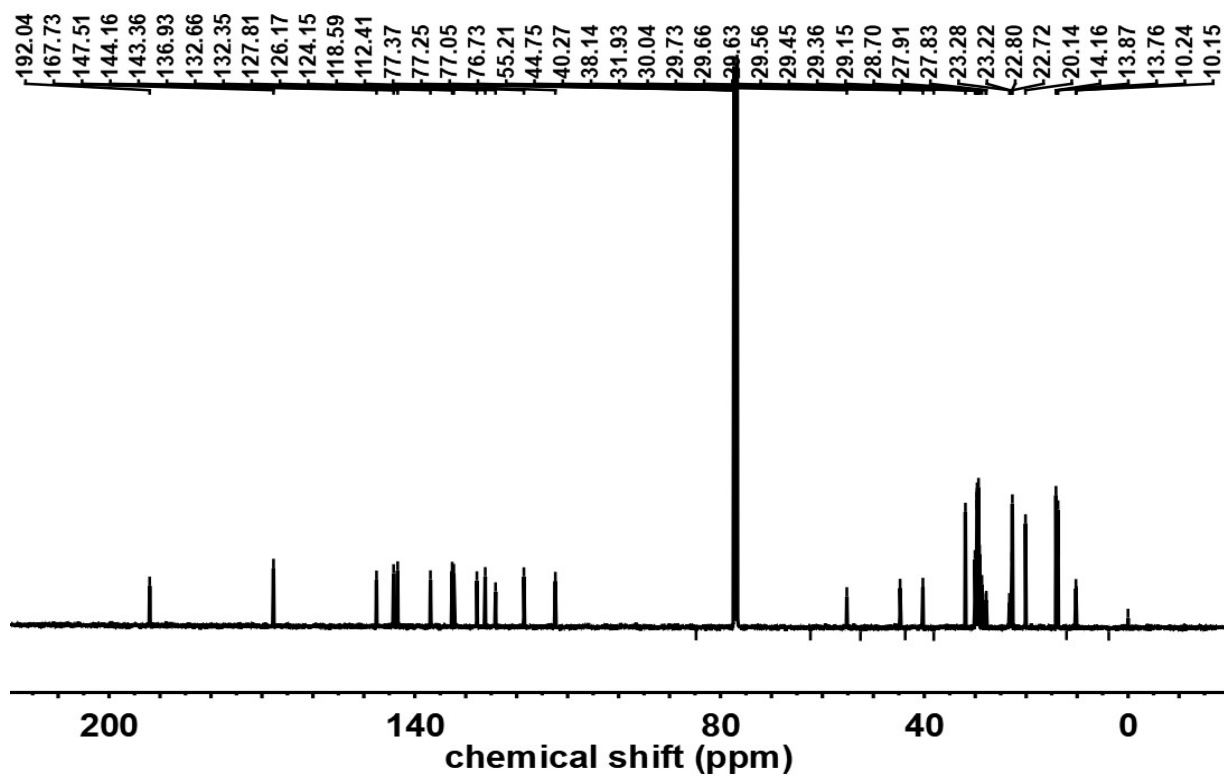


Fig. S14  $^{13}\text{C}$ NMR spectra of BPM1 in  $\text{CDCl}_3$ .

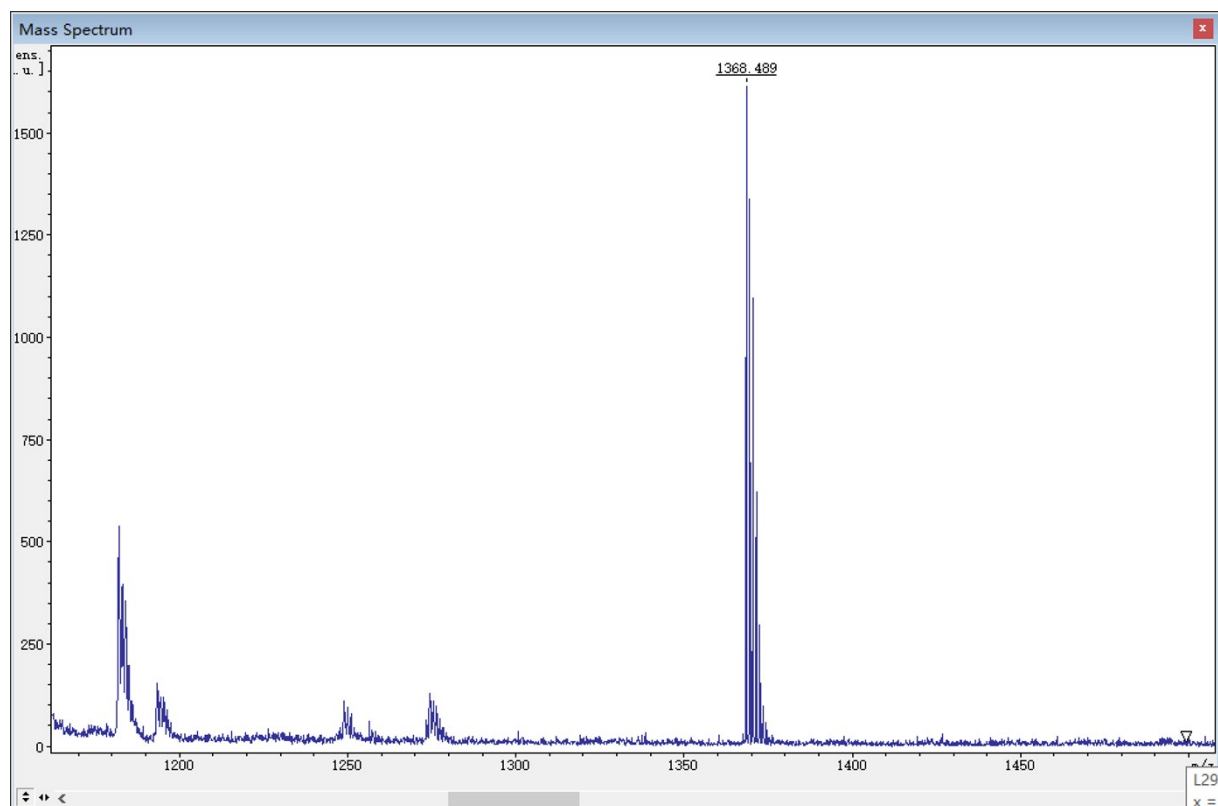


Fig. S15 MALDI-TOF spectra of BPM1 in  $\text{CHCl}_3$ .

**Table S1.** With TA 130 °C treatment for 10 min, photovoltaic parameters of **P3HT:BPM1** OSCs with different D/A weight ratios under the illumination of AM 1.5G, 100 mW cm<sup>-2</sup>.

D:A (w/w)	$V_{oc}$ (V)	$J_{sc}$ (mA cm <sup>-2</sup> )	FF (%)	PCE (%)
1.5:1	1.04	5.7	40.9	2.4
1:1	1.09	11.4	57.0	7.1
1:1.5	1.04	9.5	43.9	4.3

**Table S2.** Photovoltaic parameters of the OSCs based on **P3HT:BPM1** blend with as-cast and different TA temperature under the illumination of AM 1.5G, 100 mW cm<sup>-2</sup>.

Condition (°C)	$V_{oc}$ (V)	$J_{sc}$ (mA cm <sup>-2</sup> )	FF (%)	PCE (%)
as-cast	1.13	3.2	29.9	1.1
110	1.09	11.9	52.0	6.7
130	1.09	11.4	57.0	7.1
150	1.07	10.7	57.9	6.6

**Table S3.** With TA 130°C treatment for 10 min, photovoltaic parameters of **P3HT:BPM1** OSCs with different solvents under the illumination of AM 1.5G, 100 mW cm<sup>-2</sup>.

Solvent	$V_{oc}$ (V)	$J_{sc}$ (mA cm <sup>-2</sup> )	FF (%)	PCE (%)
Toluene	1.06	10.6	54.0	6.1
o-xylene	1.01	9.9	50.4	5.0
CF	1.06	10.7	50.1	5.7
Tetrahydrofuran	1.09	11.4	57.0	7.1

**Table S4.** With TA 130°C treatment for 10 min, photovoltaic parameters of **P3HT:BPM1** OSCs with different additives under the illumination of AM 1.5G, 100 mW cm<sup>-2</sup>.

Additives	$V_{oc}$ (V)	$J_{sc}$ (mA cm <sup>-2</sup> )	FF (%)	PCE (%)
Without additive	1.09	11.4	57.0	7.1
DIO	1.03	8.7	57.3	5.1
CN	1.04	8.2	59.9	5.1
PN	1.03	8.7	53.9	4.8
NMP	1.08	8.7	57.1	5.4
DPE	1.04	9.1	55.8	5.3

**Table S5.** Photovoltaic parameters of **BPM1:Y6** OSCs with as-cast and CS<sub>2</sub>-SVA-90 s under the illumination of AM 1.5G, 100 mW cm<sup>-2</sup>

Conditions	$V_{oc}$ (V)	$J_{sc}$ (mA cm <sup>-2</sup> )	FF (%)	PCE (%)
BPM1:Y6 <sup>a</sup>	0.89	4.4	37.8	1.5

BPM1:Y6 <sup>b</sup>	0.86	22.9	53.1	10.5
----------------------	------	------	------	------

<sup>a</sup>: as-cast; <sup>b</sup>: CS<sub>2</sub>-SVA-90 s.

**Table S6:** Photovoltaic parameters of **BPM1:Y6** OSCs with different solvents with SVA under the illumination of AM 1.5G, 100 mW cm<sup>-2</sup>.

Solvents	$V_{oc}$ (V)	$J_{sc}$ (mA cm <sup>-2</sup> )	FF (%)	PCE (%)
CS <sub>2</sub>	0.86	22.9	53.1	10.5
CHCl <sub>3</sub>	0.86	21.3	47.0	8.6
CH <sub>2</sub> Cl <sub>2</sub>	0.32	0.80	28.5	0.1

**Table S7.** Photovoltaic parameters of **BPM1:PM7:Y6** OSCs with different content of PM7 under the illumination of AM 1.5G, 100 mW cm<sup>-2</sup>.

D <sub>1</sub> :D <sub>2</sub> :A (w/w)	$V_{oc}$ (V)	$J_{sc}$ (mA cm <sup>-2</sup> )	FF (%)	PCE (%)
1:0.1:1	0.84	25.3	69.6	14.8
1:0.2:1	0.84	24.9	64.0	13.4
1:0.3:1	0.85	25.5	63.6	13.8

**Table S8.** Photovoltaic parameters of **BPM1:PM7:Y6** OSCs with different thermal time under the illumination of AM 1.5G, 100 mW cm<sup>-2</sup>.

Time (s)	$V_{oc}$ (V)	$J_{sc}$ (mA cm <sup>-2</sup> )	FF (%)	PCE (%)
60	0.84	25.6	67.5	14.5
90	0.84	25.3	69.6	14.8
120	0.84	25.2	68.5	14.5
150	0.84	25.2	66.5	14.1

**Table S9.** The  $P_{diss}$  and  $P_{coll}$  datas of BPM1, PM7, and Y6 pure film.

Active layers	$P_{\text{diss}}$ (%)	$P_{\text{coll}}$ (%)
P3HT:BPM1 <sup>a</sup>	67.0	35.6
P3HT:BPM1 <sup>b</sup>	95.0	72.7
BPM1:Y6 <sup>c</sup>	84.2	65.7
BPM1:PM7:Y6 <sup>c</sup>	95.4	85.0

<sup>a</sup> as-cast; <sup>b</sup> Thermal annealing 130 °C for 10 min; <sup>c</sup> CS<sub>2</sub>-SVA-90 s.

**Table S10.** Mobilities of pure films of BPM1 and blend films of related OSCs.

Materials	$\mu_{\text{h}}$ (cm <sup>2</sup> V <sup>-1</sup> s <sup>-1</sup> )	$\mu_{\text{e}}$ (cm <sup>2</sup> V <sup>-1</sup> s <sup>-1</sup> )	$\mu_{\text{h}}/\mu_{\text{e}}$
BPM1	$4.68 \times 10^{-4}$	$6.10 \times 10^{-4}$	
P3HT:BPM1 <sup>a</sup>	$1.78 \times 10^{-4}$	$4.69 \times 10^{-6}$	38.0
P3HT:BPM1 <sup>b</sup>	$7.75 \times 10^{-4}$	$1.25 \times 10^{-4}$	6.14
BPM1:Y6 <sup>c</sup>	$2.61 \times 10^{-5}$	$1.98 \times 10^{-5}$	1.32
BPM1:PM7:Y6 <sup>c</sup>	$5.79 \times 10^{-4}$	$4.92 \times 10^{-4}$	1.18

<sup>a</sup>: as-cast; <sup>b</sup>: thermal annealing 130 °C for 10 min; <sup>c</sup>: CS<sub>2</sub>-SVA-90 s.

**Table S11.** Summary of the  $d$ -spacing and coherence lengths of the in-plane (IP) and out-of-plane (OOP) peak for neat films.

Materials	Peak Position (Å <sup>-1</sup> )	Stacking Distance $d$ (Å)	FWHM of Peak (Å <sup>-1</sup> )	CCL of Stacking (Å)
-----------	----------------------------------	---------------------------	---------------------------------	---------------------



	IP (100)	OOP (010)	IP (100)	OOP (010)	IP (100)	OOP (010)	IP (100)	OOP (010)
P3HT	0.37	1.64	16.98	3.83	0.06	0.19	94.25	29.76
BPM1 <sup>a</sup>	0.26	1.67	24.17	3.76	0.09	0.50	62.83	11.31
BPM1 <sup>b</sup>	0.27	1.66	23.27	3.78	0.08	0.48	70.68	11.78
Y6	0.29	1.73	21.67	3.63	0.08	0.26	70.68	21.75
PM7	0.30	1.65	20.94	3.81	0.14	0.47	40.39	12.03

<sup>a</sup>The neat film in THF; <sup>b</sup> The neat film in CHCl<sub>3</sub>.

**Table S12.** Summary of the *d*-spacing and coherence lengths of the in-plane (IP) and out-of-plane (010) for P3HT:BPM1<sup>a</sup>, P3HT:BPM1<sup>b</sup>, BPM1:Y6<sup>c</sup>, BPM1:PM7:Y6<sup>c</sup> blend films.

Active layers	Peak Position (Å <sup>-1</sup> )		Stacking Distance <i>d</i> (Å)		FWHM of Peak (Å <sup>-1</sup> )		CCL of Stacking (Å)	
	IP (100)	OOP (010)	IP (100)	OOP (010)	IP (100)	OOP (010)	IP (100)	OOP (010)
P3HT:BPM1 <sup>a</sup>	0.37	1.64	16.98	3.83	0.19	0.28	29.76	20.19
P3HT:BPM1 <sup>b</sup>	0.38	1.67	16.53	3.76	0.04	0.19	141.37	29.76
BPM1:Y6 <sup>c</sup>	0.26	1.73	24.17	3.63	0.09	0.24	62.83	23.56
BPM1:PM7:Y6 <sup>c</sup>	0.26	1.72	24.17	3.65	0.10	0.26	56.55	21.75

<sup>a</sup>:as-cast; <sup>b</sup>: thermal annealing 130 °C for 10 min; <sup>c</sup> CS<sub>2</sub>-SVA-90 s.

**Table S13.** The contact angles and surface energy parameters of BPM1, PM7, and Y6 pure film.

Sample	Contact angles		$\gamma^d$ (mN·m <sup>-1</sup> )	$\gamma^p$ (mN·m <sup>-1</sup> )	$\gamma$ (mN·m <sup>-1</sup> )	$(\gamma_D^{1/2}-\gamma_A^{1/2})^2$
	$\theta_{\text{water}}$ (°)	$\theta_{\text{DIM}}$ (°)				
BPM1	98.2	35.2	43.82	0.002	43.8	0.124 $\kappa$
PM7	105.5	45.1	39.75	0.150	39.9	0.024 $\kappa$
Y6	93.8	41.5	38.81	0.476	39.3	--

- 1 C. G. Shuttle, R. Hamilton, B. C. O'Regan, J. Nelson and J. R. Durrant, *PANS*, 2010, **107**, 16448-16452.
- 2 L. Lu, T. Xu, W. Chen, J. Lee, Z. Luo, I. H. Jung, H. I. Park, S. Kim and L. Yu, *Nano Lett.*, 2013, **13**, 2365-2369.
- 3 L. Lu, W. Chen, T. Xu and L. Yu, *Nat. Commun.*, 2015, **6**, 7327.
- 4 V. D. Mihailetschi, L. J. A. Koster, J. C. Hummelen, P. W. M. Blom, *Phys. Rev. Lett.*, 2004, **93**, 216601.
- 5 V. D. Mihailetschi, J. Wildeman, P. W. M. Blom, *Phys. Rev. Lett.*, 2005, **94**, 126602.
- 6 R. Barla, B. Lochab, A. Agrawal, A. Mishra, M. L. Keshtov and G. D. Sharma, *Sol. RRL*, 2021, **5**, 2100402.
- 7 D. M. Smilgies, *J. Appl. Cryst.*, 2009, **42**, 1030-1034.
- 8 D. Qian, Z. Zheng, H. Yao, W. Tress, T. R. Hopper, S. Chen, S. Li, J. Liu, S. Chen, J. Zhang, X. K. Liu, B. Gao, L. Ouyang, Y. Jin, G. Pozina, I. A. Buyanova, W. M. Chen, O. Inganas, V. Coropceanu, J. L. Bredas, H. Yan, J. Hou, F. Zhang, A. A. Bakulin and F. Gao, *Nat Mater.*, 2018, **17**, 703-709.